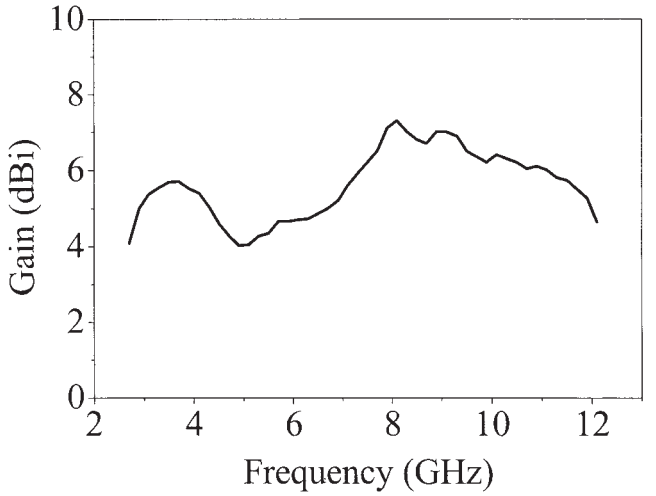

Figure 5 Measured antenna gain vs. frequency for the proposed antenna studied in Fig. 2

and y–z planes at 3, 5.3, 7.9, and 10 GHz are plotted in Figure 4. It is observed that the radiation patterns at the lower frequencies (3 and 5.3 GHz) are not much different. Conversely, the copolarized components of the x–z plane at the higher frequencies (7.9 and 10 GHz) are relatively distorted due to the generation of the higher order modes and an offset rectangular stub with respect to the y-axis. Figure 5 presents the measured antenna gain versus frequency. The antenna gain varies from about 4 to 7.3 dBi over the impedance bandwidth obtained.

4. CONCLUSION

An ultra-wideband square-slot antenna fed by an offset rectangular microstrip line has been proposed and successfully implemented. The measured impedance bandwidth of the antenna is from 2.78 to 12.02 GHz for VSWR < 2. This antenna is suitable for application in UWB systems.

ACKNOWLEDGMENT

This work was sponsored by the National Science Council, R.O.C., under contract no. NSC 93-2213-E-230-006.

REFERENCES

1. C. Ying and Y.P. Zhang, Integration of ultra-wideband slot antenna on LTCC substrate, Electron Lett 40 (2004), 645–646.
2. Y.W. Jang, Experimental study of a large bandwidth rectangular microstrip-fed circular slot antenna, Microwave Opt Technol Lett 33 (2002), 316–318.
3. G. Sorbello, F. Consoli, and S. Barbarino, Numerical and experimental analysis of a circular slot antenna for UWB communications, Microwave Opt Technol Lett 44 (2005), 465–470.
4. C. Ying, G.Y. Li, and Y.P. Zhang, An LTCC planar ultra-wideband antenna, Microwave Opt Technol Lett 42 (2004), 220–222.
5. T.G. Ma and S.K. Jeng, Planar miniature tapered-slot-fed annular slot antennas for ultrawide-band radios, IEEE Trans Antennas Propagat AP-53 (2005), 1194–1202.

H-PLANE 3-dB HYBRID RING OF HIGH ISOLATION IN SUBSTRATE-INTEGRATED RECTANGULAR WAVEGUIDE (SIRW)

Wenquan Che,[1,2] Kuan Deng,[1] Edward K. N. Yung,[2] and Ke Wu[3]
[1] Department of Electrical Engineering
Nanjing University of Science & Technology
Nanjing, P.R. China
[2] Department of Electronic Engineering
City University of Hong Kong
83 Tat Chee Avenue, Kowloon
Hong Kong, P.R. China
[3] Poly-Grames Research Center
Ecole Polytechnique de Montreal
Montreal, Canada

Received 29 August 2005

ABSTRACT: *An H-plane hybrid ring 3-dB power divider constructed with substrate integrated rectangular waveguide (SIRW) is proposed. Theoretical simulations are carried out at the X- and Ka-bands. The results show that the isolation between two output ports is high up to 35 dB and good 3-dB power division within the band of interest is observed also, that is, less than 0.3-dB derivation in the band of interest. In addition, the simulation results at the X-band shows a bandwidth of 10% at −15 dB. A prototype in the Ka-band is fabricated and the measured data at the Ka-band shows a bandwidth of 7% at −15 dB, in good agreement with simulation.* © 2006 Wiley Periodicals, Inc. Microwave Opt Technol Lett 48: 502–505, 2006; Published online in Wiley InterScience (www.interscience.wiley.com). DOI 10.1002/mop.21392

Key words: *H-plane 3-dB hybrid ring; substrate integrated rectangular waveguide (SIRW)*

1. INTRODUCTION

It has been known that the waveguide power dividers, such as the hybrid ring, are building blocks of many microwave and millimeter-wave integrated circuits and systems [1]. The very low power loss of the rectangular waveguide allows the design of high-Q components. Since the fabrication cost of rectangular waveguide structure can be high, the hybrid ring can also be implemented in microstrip with much lower cost. Unfortunately, the microstrip hybrid has a power capacity and a Q factor too low to be of use in many applications.

To overcome those drawbacks of high cost or low Q, a new design platform has been proposed. This new hybrid is in substrate-integrated rectangular waveguide (SIRW) [2–4], that is, it is synthesized in a planar substrate with arrays of metal vias forming the waveguide walls. Many innovative components have been constructed in SIRW [5–7] and have been found to provide unique performance in hybrid microwave and millimeter-wave integrated circuits. The SIRW combines the advantages of rectangular waveguide and microstrip, that is, they have the higher Q factor and power capacity of a waveguide but the low cost, low profile, small volume, and lighter weight of a microstrip.

In this paper, an H-plane 3-dB hybrid ring constructed in SIRW is proposed and investigated at two frequencies: the X-band and the Ka-band. The hybrid ring may share the same substrate with the microstrip transition if the hybrid ring is to be connected to microstrip circuits. The simulated results in the X-band indicate a bandwidth of 10% at −15 dB return loss. A Ka-band prototype has been fabricated and measured. The experiment shows bandwidth of 7% at −15 dB in the Ka-band. It also shows a high isolation between two output ports up to 35 dB, no resistor is required to

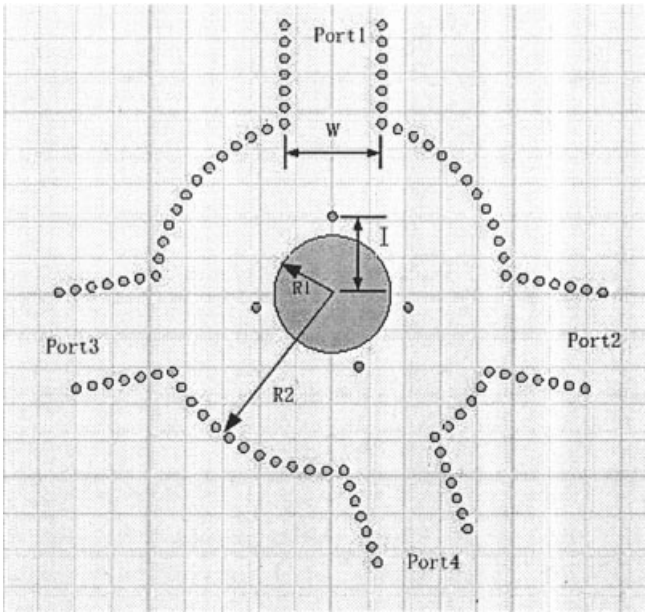

Figure 1 Schematic top view of the H-plane hybrid ring based in SIRW

improve the isolation. Obviously, the bandwidth is narrower than that of the microstrip hybrid rings, some improvements are still required to improve the bandwidth. However, the Q factor and the power-handling capacity of the SIRW hybrid ring are higher. With the features of planar structure and low profile, this device is expected to incorporate into the design of hybrid microwave integrated subsystems.

2. STRUCTURE OF HYBRID RING 3-dB POWER DIVIDER

As we know, the hybrid ring can usually be implemented in form of microstrip, coaxial line, stripline, and/or waveguide. The waveguide hybrid ring takes the feature of relatively high power capacity; however, this device is difficult to integrate with planar circuits, as complex transition from waveguide to planar transmission lines is required. In this way, a hybrid ring constructed in a substrate-integrated rectangular waveguide is proposed. Figure 1 shows the top view of the H-plane hybrid ring in SIRW.

2.1. Dimensions of Four Arms

The dimensions of the SIRW are selected based on references [3], including the diameters of the metal posts, the pitch between two posts, the widths of the arms and the ring, and so forth. It should be noted that the width of the four arms depends on the consideration that only the dominant mode TE_{10} can propagate in the SIRW, the cutoff frequencies of TE_{10} and TE_{20} modes in SIRW can be found from [8]. In addition, the propagation constant of the TE_{10} mode in a rectangular waveguide is only related to the width; the height of the waveguide has nearly no effect. The thickness of the substrate can therefore be reduced significantly without much influence on the propagation of the TE_{10} mode in the SIRW. In this way, the parameters and the dimensions of the SIRW arms are given as below. In the Ka-band, the thickness of the substrate is $h = 0.035\lambda_0$, the relative permittivity $\varepsilon_r = 2.33$; the diameter of the metal posts is chosen as $D = 0.070\lambda_0$, while the spacing of the adjacent posts is $P = 0.123\lambda_0$, and the width of the SIRW is $W = 0.737\lambda_0$. In the X-band, the thickness of the substrate is $h = 0.03\lambda_0$ and the relative permittivity $\varepsilon_r = 10.2$, the diameter of the metal posts is chosen as $D = 0.070\lambda_0$, while the spacing of the adjacent posts is $P = 0.129\lambda_0$ and the width of the SIRW is $W = 0.707\lambda_0$.

2.2. Width of Ring

According to the design principle of the hybrid ring, the width of the ring $(R_2 - R_1)$ has the following relationship with the width of four arms, that is:

$$\frac{W'}{W} = \frac{R_2 - R_1}{W} = \sqrt{2 - \left(\frac{\lambda_0}{2W}\right)^2}, \tag{1}$$

where R_2 and R_1 are the outer and inner radii of the hybrid ring, respectively, λ_0 is the wavelength in free space at center frequency, and W is the known width of the four arms. Figure 2 illustrates the generalized guided wavelength in the ring versus frequency. It has been found that the bandwidth of the hybrid ring greatly depends on the change of the guided wavelength with frequency. Obviously, the change of the guided wavelength is rather abrupt in the lower part of the frequency range; it is quite difficult to achieve a good match in a broad band. Therefore it is reasonable to choose the operational frequency and related guided wavelength in the smooth range to obtain a good match. However, the operation frequency cannot be chosen at the upper limit of the range, for it is close to the emergence of TE_{20} mode. It should be noted that the central cylinder of the junction is a metal pole, forming naturally the inner sidewall of the SIRW hybrid ring.

2.3. Distances between Four Arms

The distance choice between the four arms lies on the fact that, when the arm 1 is the input port, the arms 2 and 3 should be the in-phase output ports, while the arm 4 is the isolated port. In this way, the arc length between arms 1 and 2, 1 and 3, and 3 and 4 all should be $\lambda_g/4$, while the arc length between arms 2 and 4 should be $3\lambda_g/4$. However, it is difficult to deposit three arms 1, 2, and 3 within the arc length $3\lambda_g/4$. For the sake of the practice, one wavelength has been added and the arc length $\lambda_g/4$ is thus $5\lambda_g/4$; while the distance between arms 2 and 4 remains $3\lambda_g/4$. Because of the period of one wavelength, it seems that no effect has been introduced into the simulation results at the center frequency, but the bandwidth would be affected slightly. Based on above consideration, the spatial angles between arms 1 and 2, arms 1 and 3, and arms 3 and 4, are all 100°, while the angle between arms 2 and 4 is 60°.

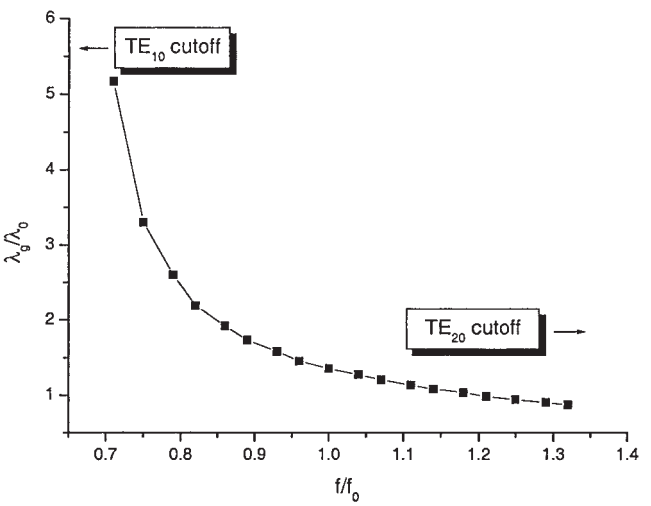

Figure 2 Dependence of guided wavelength on frequency

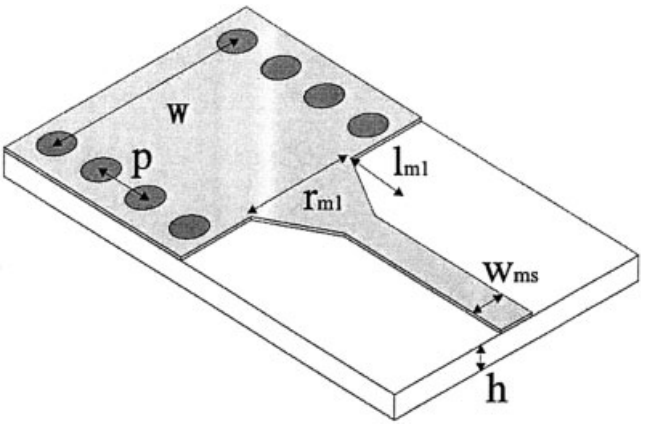

Figure 3 Schematic geometry of the microstrip transition

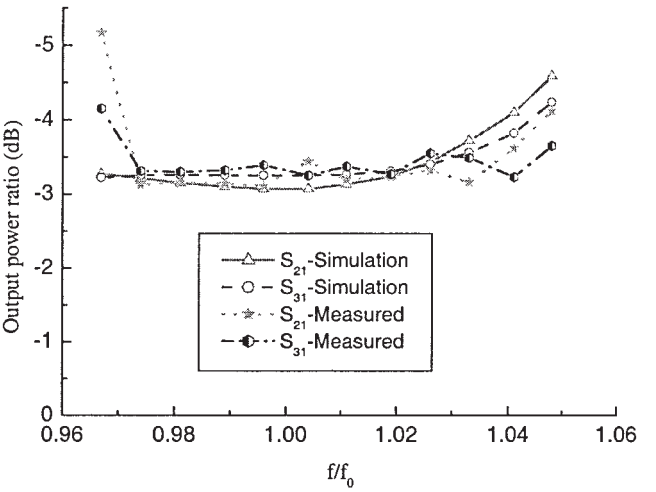

Figure 5 Experimental and simulated power ratio in the Ka-band

3. IMPEDANCE MATCHING

It is generally required to have a relative broad band within which good VSWR, equal power ratio, and high isolation can be expected. In this project, a simple technique has been employed to increase the bandwidth, that is, a metallized pole has been deposited along the axis of each arm as illustrated in Figure 1; with space I to the center of the H-plane hybrid ring. With these four metal posts in the ring, inductances are introduced and then cancel the capacitances existing between the outer and inner sidewalls, thus improving the bandwidth. It should be noted that the inner radius of the ring should be decreased a bit after the four-metallized poles were introduced in order to achieve good match. In addition, the two posts of each arm close to the ring should be removed; in this case, a step impedance-matching section is introduced between the arm and the ring in order to further improve the bandwidth. In addition, one simple transition from SIRW to microstrip line is required for the purpose of measurement or integration with other planar circuits [3]. The schematic geometry of the transition is illustrated in Figure 3, where W is the width of the four arms of the hybrid ring, w_{ms} is the width of the 50Ω microstrip, and l_{ml} is the length of the transition.

4. RESULTS AND DISCUSSION

At the X-band, the center frequency is $f_0 = 10$ GHz. The width of the ring is chosen as $W' = 0.707\lambda_0$, the generalized guided wavelength of the ring is $\lambda_g/\lambda_0 = 1.419$, and the inner and outer radii of the hybrid ring are $R_1 = 0.423\lambda_0$ and $R_2 = 0.423\lambda_0$, respectively. The position of the four matching posts is given as $l = 0.141\lambda_0$. The simulated return loss and isolation are illustrated in Figure 4, while the power output ratio at ports 2 and 3 are also shown in Figure 4. Obviously, the input power at port 1 is divided equally at ports 2 and 3; less then 0.25-dB difference has been observed in the whole band of interest. In addition, good isolation up to 35 dB can be obtained between arms 1 and 4. The bandwidth is about 10% less than −15 dB.

At the Ka-band, the center frequency is $f_0 = 27$ GHz. The width of the ring is $W' = 0.737\lambda_0$, while the generalized guided wavelength of the ring is $\lambda_g/\lambda_0 = 1.428$. The inner and outer radii of the hybrid ring are $R_1 = 0.423\lambda_0$ and $R_2 = 0.423\lambda_0$, respectively. The position of the four matching posts is $l = 0.179\lambda_0$. In addition, for the purpose of measurement, one microstrip transition is introduced with dimensions $w_{ms} = 0.098\lambda_0$, $r_{ml} = 0.337\lambda_0$, and $l_{ml} = 0.804\lambda_0$. The simulated power output ratio of arms 2 and 3 are illustrated in Figure 5, the return loss and isolation are given in Figure 6. The results show about 7% bandwidth with less than −15 dB return loss. In addition, the high isolation between arms 1 and 4 and arms 2 and 3 can be observed,

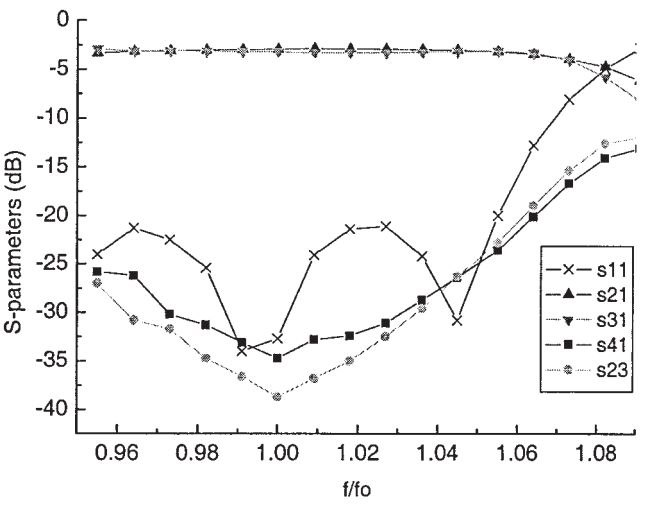

Figure 4 Simulated return loss, isolation, and power ratio in the X-band

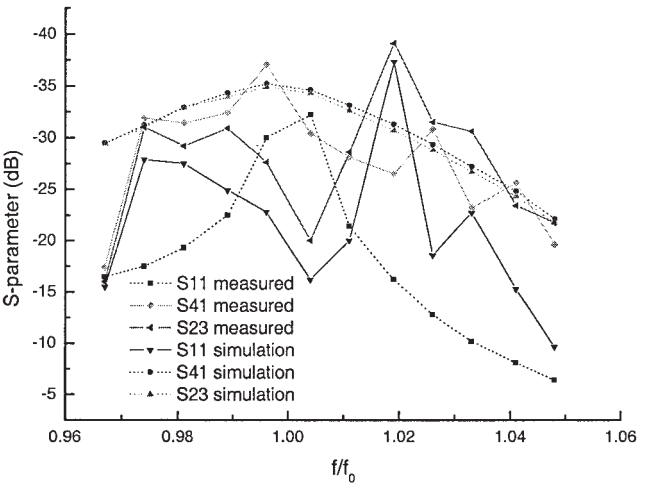

Figure 6 Experimental and simulated return loss and isolation in the Ka-band

all nearly more than 25 dB in the band of interest. In order to verify the validity of the theoretical expectation, one prototype at the Ka-band has been fabricated and measured; all the data have also been illustrated in Figures 5 and 6. Obviously, good agreement has been observed between the simulation and the experiment; especially, the high isolation between the two output ports is quite remarkable—more than 25 dB in the band of interest. The derivation of measured output power is larger (about 0.45 dB) than the simulation results in the upper-frequency range, although the VSWR is better. In addition, the measured isolations S_{41} and S_{23} have some fluctuation in the band (especially the upper part), which is probably due to the fact that the measured results include the contribution of the microstrip transition, which will inevitably affect the isolation and the output power ratio. In addition, the measured return loss is worse than the simulation due to the microstrip transition. Undoubtedly, some optimization is still required to obtain the optimum results.

5. CONCLUSION

In this letter, an H-plane hybrid ring constructed in substrate-integrated rectangular waveguide (SIRW) has been presented and some design techniques have been introduced. Good performances have been observed from the simulation and experiments, especially high isolation between the two output ports. Compared with the rectangular waveguide hybrid ring, this structure takes advantage of low cost, low profile, small volume, and ease of integration. However, the bandwidth is narrower than that of the microstrip hybrid rings although the Q factor of the SIRW hybrid ring is higher; some improvements are still required to increase the bandwidth. In any case, with the features of a planar structure and low profile, this device is expected to be incorporated in designs of hybrid microwave integrated subsystems.

ACKNOWLEDGMENT

The authors would like to express their gratitude for the financial support of the National Science Foundation of China under grant no. 60471025 and the Natural Science Foundation of Jiangsu Province under grant no. BK2004135.

REFERENCES

1. D.M. Pozar, Microwave engineering, 2nd ed., Wiley, New York, 1998.
2. J. Hirokawa and M. Ando, Single-layer feed waveguide consisting of posts for plane TEM wave excitation in parallel plates, IEEE Trans Antennas Propagat AP-46 (1998), 625–630.
3. D. Deslandes and K. Wu, Integrated microstrip and rectangular waveguide in planar form, IEEE Microwave Wireless Compon Lett 11 (2001), 68–70.
4. K. Wu, Integration and interconnect techniques of planar and nonplanar structures for microwave and millimeter-wave circuits-current status and future trend, Proc Asia-Pacific Microwave Conf, Taipei, Taiwan, R.O.C. (2001), 411–416.
5. Y.L. Zhang, W. Hong, K. Wu, et al., Novel substrate integrated waveguide cavity filter with defected ground structure, IEEE Trans Microwave Theory Tech MTT-53 (2005), 1280–1287.
6. Y. Cassivi and K. Wu, Low-cost microwave oscillator using substrate integrated waveguide cavity, IEEE Microwave Wireless Compon Lett 13 (2003), 48–50.
7. Y. Li, W. Hong, T.J. Cui, K. Wu, et al., Simulation and experiment on SIW slot array antennas, IEEE Microwave Wireless Compon Lett 14 (2004), 446–448.
8. Y. Cassivi, L. Perregrini, P. Arcioni, M. Bressan, K. Wu, and G. Conciauro, Dispersion characteristics of substrate integrated rectangular waveguide, IEEE Microwave Wireless Compon Lett 12 (2002), 333–335.

CIRCULAR MICROSTRIP ANTENNA WITH A SECTOR-SLOT FOR DUAL-PORT OPERATION

Deepti Das Krishna, C. K. Aanandan, P. Mohanan, and K. Vasudevan
Centre for Research in Electromagnetics and Antennas
Department of Electronics
Cochin University of Science & Technology
Cochin 682022, India

Received 25 August 2005

ABSTRACT: *Design of a dual-port circular patch antenna with a sector-slot for dual-frequency operation is presented. The antenna resonates at two distinct frequencies with orthogonal polarizations and broad radiation characteristics. Unlike the conventional circular patch, this antenna can be microstrip-fed to operate at either of the resonances. The two polarizations can be simultaneously excited using two electromagnetically coupled ports with an isolation better than −30 dB between the ports. This antenna has the added advantage of size reduction of 44% compared to the conventional circular patch without any reduction in gain.* © 2006 Wiley Periodicals, Inc. Microwave Opt

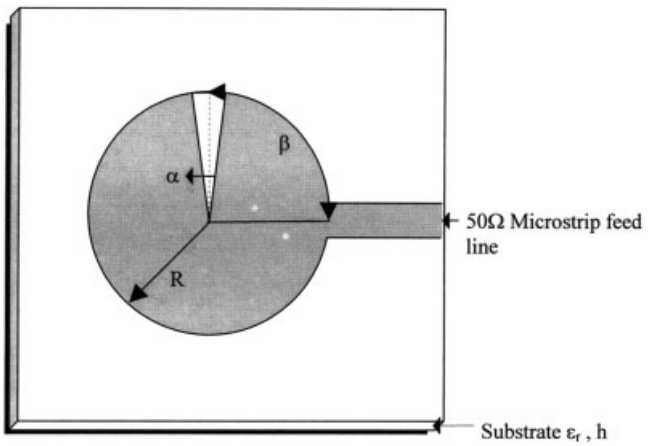

Figure 1 Geometry of the microstrip-fed circular patch antenna with a sector slot

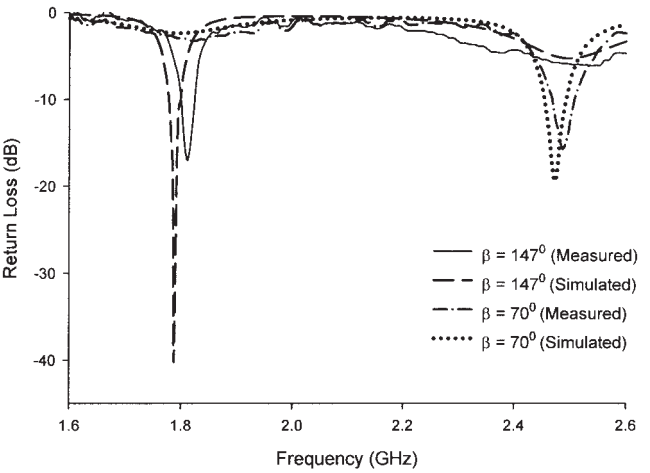

Figure 2 Measured and simulated return losses (S_{11}) for the microstrip fed circular patch antenna with a sector slot $R = 17.5$ mm, $\alpha = 20°$, $\varepsilon_r = 4.36$, and $h = 1.6$ mm